Journal of Information and Computing Science
J. Info. Comput. Sci., Vol. 18, No. 1, pp. 51-66

DOI: 10.4208/JICS-2023-004
June 2023

An Algorithm for 3D Modeling of Doppler Weather Radar Base Data

Xiaoru Yin[1,2], Shengming Jiao[1,*], Du Xi[3] and Tingting Bao[1]

[1] *Jiangsu Meteorological Information Center, Nanjing 210088, China;*
[2] *Key Laboratory of Transportation Meteorology, China Meteorological Administration, Nanjing 210008, China;*
[3] *Jiangsu Meteorological Observatory, Nanjing 210008, China*

Abstract. This paper proposed a Marching Trapezoidal Polyhedrons 3D modeling algorithm (MTPD) based on the cone-shaped spatial distribution of Doppler weather radar base data. In this algorithm, a trapezoidal polyhedron was introduced to replace the cube in the conventional modeling algorithm as a basic volume element for modelling. On the other hand, the hexahedral index or tetrahedral index was selected as the construction model for the 3D iso-surface based on the difference in spatial range for 3D radar modeling, to balance the efficiency of the algorithm and the precision of the modeling results. Based on this algorithm, a Doppler weather radar 3D visualization platform was developed using WebGL technology. The results revealed that the algorithm significantly improved efficiency without compromising the precision of 3D modeling when compared with the conventional modeling algorithm based on radar grid data. The durations for the algorithms were reduced by 1.9 seconds and 0.7 seconds, respectively under the hexahedral index mode and the tetrahedral index mode, while under the tetrahedral index mode, the 3D echo structure was more continuous with a higher level of precision. The Doppler weather 3D radar visualization platform based on the B / S architecture could provide a cross-platform 3D radar display, thus visualize the 3D structure of convective cloud effectively.

AMS subject classifications: 68Q25, 93A30
Key words: Doppler weather radar, 3D modeling, Marching trapezoidal polyhedrons, WebGL.

1 Introduction

Translated from *Journal of Nanjing University of Information Science & Technology*, 2023, 15(1): 111-120.
*Corresponding author. *Email addresses:* **yxr_vicky@163.com** (X. Yin), **jandyjsm@126.com** (S. Jiao).

Doppler weather radar is one of the main means to detect mesoscale convective weather systems and their intensity, distribution, development and evolution. With high temporal and spatial resolution, Doppler weather radar plays an important role in improving the accuracy of severe weather warning and prediction [1-4]. It is an intuitive and effective means for meteorologists to observe the distribution and development of radar echoes and analyze weather process accurately by using computer graphics technology to display the base data generated by weather radar detection. At present, the display of weather radar data used in meteorological services in China is still dominated by two-dimensional images [5-7], but the two-dimensional display mode only reflects the distribution of echoes at a certain level, which is difficult to truly reflect the spatial structure of the cloud. 3D modeling can intuitively display and analyze the internal characteristics of radar echoes, which is helpful to understand the spatial structure of weather system and improve the forecasting ability of weather system. Therefore, 3D modeling of weather radar data is an inevitable trend of meteorological data application, and it is also an urgent need for the development of weather forecasting business.

In recent years, domestic and foreign scholars have carried out relevant research on the three-dimensional modeling of weather radar. Ernvik [8] used three algorithms of cross-section plane slice, surface extraction and stereo rendering to conduct three-dimensional modeling research on radar echoes. Kristof et al. [9] realized three-dimensional display of NEXRADII reflectivity data by CUDA ray-casting algorithm for core stereoscopic rendering. Moreno et al. [10] combined two-dimensional images of radar reflectance at each elevation Angle of radar as input to form a three-dimensional radar echo structure. Xiao et al. [11] used NVI algorithm to interpolate radar reflectance data into three-dimensional grid points of latitude and longitude. Zhang Zhiqiang et al. [12] used moving cube algorithm and ray projection algorithm to realize three-dimensional reconstruction of radar echo on this basis, and the product was applied in the Short Time Approaching Forecast System of catastrophic weather (SWAN). Luo [13] uses Proximity Clouds algorithm to improve the light projection algorithm to achieve three-dimensional radar display. Han [14] realized three-dimensional modeling of radar echoes by extracting the contour lines of PPI image faults of weather radar. The above visualization algorithms extend the radar echo display from a two-dimensional plane to a three-dimensional space, which is conducive to the in-depth analysis of radar data, but there are still certain limitations. 1) he above algorithms all use regular grid data as the data source of radar echo 3D modeling, requiring the radar base data stored in the form of polar coordinates to be interpolated into the three-dimensional grid points under the Cartesian coordinate system. Although this improves the spatial accuracy of radar data, it consumes a lot of computing resources on the one hand, and makes the visualization accuracy depend on the accuracy of the interpolation algorithm on the other hand. 2) Because the amount of 3D grid data obtained by interpolation is much larger than that of the original radar data, the calculation is more complicated, reducing the efficiency of the algorithm, and it is difficult to adapt to the scene with high real-time interaction

requirements.

In general, the traditional radar 3D modeling algorithm based on interpolation grid data has many defects such as preprocessing, high computational complexity, and large amount of rendered data, so it cannot be applied to real-time services requiring fast response. At present, the mainstream radar 3D display systems at home and abroad, such as domestic SWAN system, foreign Vis5D and GR2analyst, all adopt C/S architecture, and the application range of such systems is limited due to different installation requirements [15-16]. In this paper, the Marching Trapezoidal Polyhedrons 3D modeling algorithm (MTPD) is proposed based on the data characteristics of Doppler weather radar base data as the data source. Compared with traditional 3D modeling algorithm, the accuracy and applicability of the proposed algorithm are evaluated. On the basis of MTPD algorithm, a 3D visualization platform of Doppler weather radar based on B/S architecture was developed by using WebGL technology, and the severe convective weather in Nanjing on March 20, 2019 was analyzed.

2 Doppler weather radar base is introduced

The observation method of Doppler weather radar firstly takes the radar station as the origin at an elevation Angle and carries out 360° scanning and sampling clockwise from its due north direction to obtain the data on the scanning cone, and then scans the specified elevation Angle one by one from low to high according to different volume scanning methods [17]. After completing a body scan, the radar uses elevation Angle, azimuth Angle and radial distance as the coordinate origin to store radar reflectivity, spectral width and radial velocity, and generates a binary base data file [18]. Since the reflectance factor in Doppler weather radar base data can directly reflect the scale and density distribution of precipitation particles inside the cloud, this paper carries out three-dimensional modeling based on the reflectance of radar base data. Figure. 1 shows the scanning mode of VCP21 of SA Doppler weather radar in precipitation weather. Nine scanning elevation angles are specified. The sampling interval of azimuth Angle on each elevation layer is 1°, the sampling interval of adjacent samples along the radial direction is 1 km, the maximum detection distance is 460 km, and the interval of body scanning is 6 min.

3 3D modeling algorithm MTPD

The MTPD algorithm idea (Figure 2) is as follows.

1) Voxel construction: in 3D modeling theory, the minimum processing volume unit is called voxel [19], and MTPD uses trapezoidal hexahedral as voxel to construct three-dimensional structure of radar base data.

2) Determination of applicable mode: according to the size of the modeling space, one of the hexahedral index and tetrahedral index is selected to construct

three-dimensional iso-surface to balance the efficiency of the algorithm and the accuracy of the result.

3) Calculate the intersection of iso-surface and voxel: calculate the intersection coordinates of iso-surface and voxel by interpolation method.

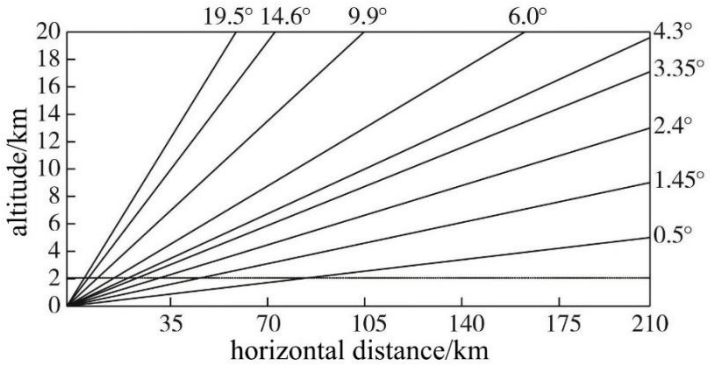

Figure 1: Elevation angle detection of CINRAD/SA Doppler weather radar VCP21

4) Drawing three-dimensional iso-surface: drawing the iso-surface in voxels one by one with the basic geometric elements of the connecting intersection points of the triangular surface, and finally obtaining the three-dimensional model of the radar echo.

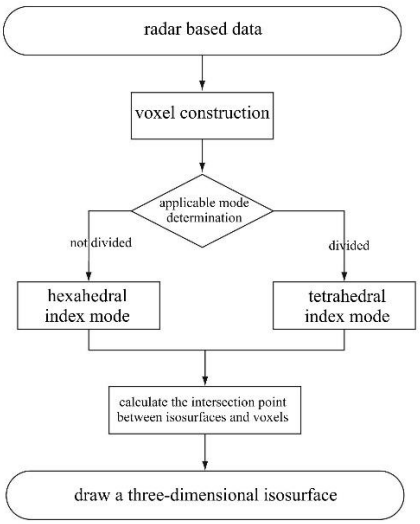

Figure 2: MTPD algorithm flow

3.1 Voxel construction

In this paper, voxels are constructed directly from polar coordinates according to the storage characteristics of radar base data, and the results are shown in Figure 3. The trapezoidal hexahedral is taken as voxel V_i by taking the length r_0 of the radial distance library, the lines of adjacent azimuths φ_i and φ_{i+1} at the same elevation and radial distance, and the lines of adjacent elevation angles θ_i and θ_{i+1} at the same azimuth and radial distance as edges respectively.

In order to facilitate the implementation of the algorithm, it is necessary to convert the polar coordinate system of the radar base data into a rectangular coordinate system with the radar station as the origin, the radar station due north direction as X forward, the radar station due west direction as Y forward, and the height from low to high as Z forward. At the same time, the echo height value is considered to be affected by the curvature of the earth [20], and the coordinate conversion formula is as follows:

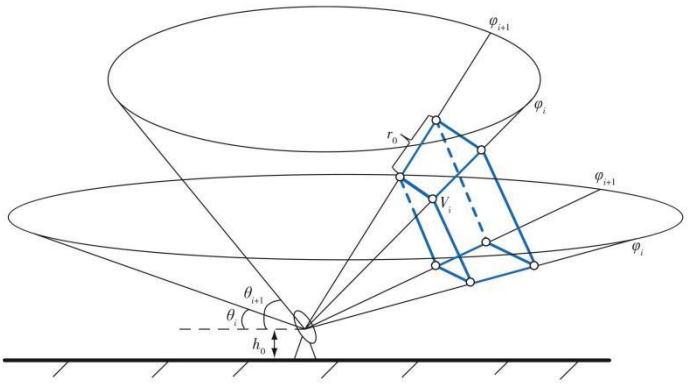

Figure 3: Constructing trapezoidal hexahedral voxels from radar base data

$$\begin{cases} x = r \times \cos\theta \times \cos\varphi, \\ y = r \times \cos\theta \times \sin\varphi, \\ z = h_0 + r \times \sin\theta + \dfrac{r^2}{2R_e}, \end{cases} \tag{1}$$

where r is the radial distance, θ is the elevation Angle, φ is the direction Angle, h_0 is the height of the radar station, and R_e is the radius of the Earth under standard atmospheric refraction.

Figure 4 shows the number of voxel vertex $V_i(0 \le i \le 7)$ and edge $E_i(0 \le i \le 11)$ in the rectangular coordinate system. The number of vertices and edge mentioned in the following Figure is an example.

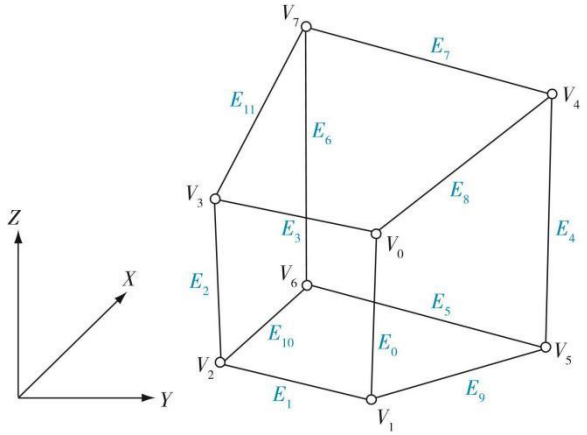

Figure 4: Vertex and edge numbering of voxels

3.2 Determination of applicable mode

The iso-surface value is α, the reflectivity of each voxel vertex has two states greater than α or less than or equal to α, and the state value is λ. Obviously, when the two endpoints λ of a voxel edge are unequal, the edge must intersect with the iso-surface. In this paper, the triangular surface is used as the basic element to connect the intersection points. As shown in Figure 5, if the two diagonal vertices λ on the surface $V_0V_3V_7V_4$ are equal and not equal to the adjacent vertices λ, there are two equivalent surface extraction methods in Figure 5a and 5b on the surface. If this surface is a common surface of adjacent voxels, the constructed three-dimensional structure will appear unclosed as shown in Figure 5c. In order to solve the above problems, the trapezoidal hexahedral is divided into 5 tetrahedral, and the equivalent surface is extracted from each tetrahedral. Figure 6 shows the topology of extracting iso-surface in tetrahedral. When all vertex state values λ are equal, there is no intersection point between tetrahedral and iso-surface (Figure 6a). Only one vertex is not equal to the λ of other vertices, resulting in a triangular surface (Figure 6b); when two vertices are not equal to the λ of the other vertices, two triangular surfaces are generated (Figure 6c). There are only three kinds of topological relations between tetrahedral and iso-surface, so there is no common surface when extracting iso-surface and there are two kinds of connection methods.

Since voxel partitioning will inevitably increase the number of voxels processed and thus increase the calculation time of the algorithm, the balance between the efficiency of the algorithm and the accuracy of the result must be considered. In this paper, the modeling method without voxel division is called hexahedral index mode, and the modeling method with voxel division is called tetrahedral index mode. Assuming that the maximum radial distance is 460 km, the maximum azimuth is 360°, and the value of each sampling point of the radar base data in the space range of 9 elevation angles is greater than 0, the time spent in generating voxels by the two modeling methods is calculated according to the 23 test space ranges given in Table 1. Figure 7 is a schematic diagram of the XY plane of the test space range selected in Table 1. $\Delta\varphi$ is the included Angle between two azimuth angles φ_i and φ_j. The radial distance of sampling points p_i and q_j is equal to r. The test space XY plane takes the fan S_{poq} composed of the origin O, p_i and q_j, and the height takes all the elevation angles.

Figure 8 shows the results of voxel construction time of the two modes in the test space range. It can be seen that the calculation time gap between the hexahedral index mode and the tetrahedral index mode is obvious in a large space, and the time of the tetrahedral index mode is twice that of the hexahedral index mode in the maximum space range. The time difference between tetrahedral index mode and hexahedral index mode is reduced to 53 ms when r is 140 km and $\Delta\varphi$ is 105° (No. 17). At this time, the S_{poq} area is about 17 959 km2. When the space range is further reduced, the calculation time difference between the two modeling methods to

generate voxels is less than 20 ms, which is almost negligible. In this paper, when implementing the algorithm, a rectangular frame is used to frame the range on the *XY* two-dimensional plane of the radar for 3D modeling. The space range is rectangle *S* on the *XY* plane and the height is all elevation angles, as shown in Figure 9. Therefore, when the rectangular *S* area is less than or equal to 17 959 km², tetrahedral index mode with higher modeling accuracy is selected, and when the rectangular *S* area is greater than 17 959 km², hexahedral index mode with faster modeling speed is selected.

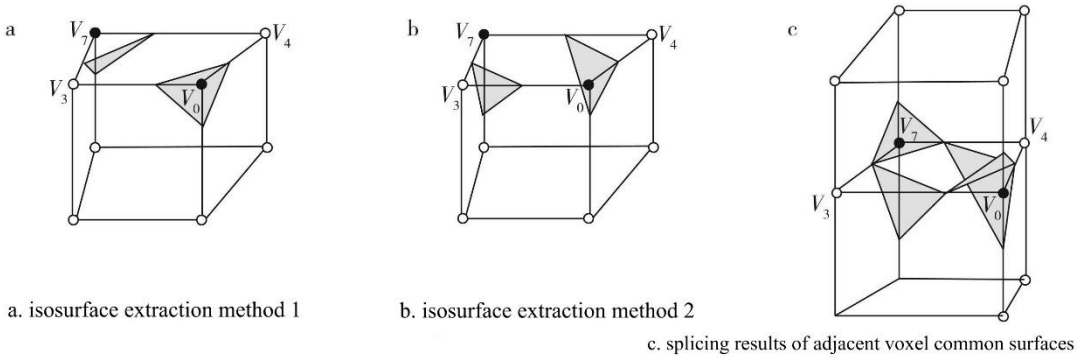

Figure 5: Iso-surface extraction topologies of adjacent voxels (hollow dots indicate that the reflectivity of the vertex is greater than α, and solid points mean that the reflectivity of the vertex is less than or equal to α)

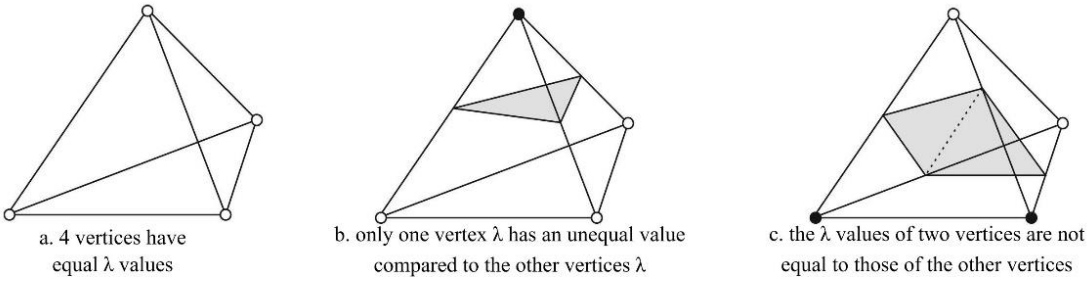

Figure 6: Iso-surface extraction topology in tetrahedral

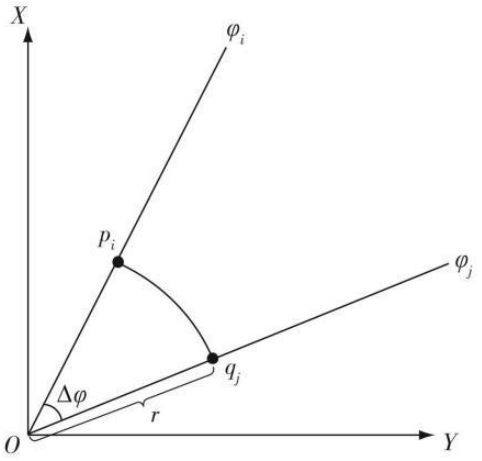

Figure 7: Schematic diagram of XY plane for test space range

Table 1: Spatial range of applicable mode test for 3D radar modeling

number	r/ km	Δφ/ (°)	S_{poq}/ km²	number	r/ km	Δφ/ (°)	S_{poq}/ km²
1	460	345	637 062.6	13	220	165	69 691.0
2	440	330	557 528.0	14	200	150	52 359.8
3	420	315	484 904.8	15	180	135	38 170.3
4	400	300	418 879.0	16	160	120	26 808.2
5	380	285	359 136.4	17	140	105	17 959.4
6	360	270	305 362.8	18	120	90	11 309.7
7	340	255	257 244.1	19	100	75	6 544.9
8	320	240	214 466.1	20	80	60	3 351.0
9	300	225	176 714.6	21	60	45	1 413.7
10	280	210	143 675.5	22	40	30	418.8
11	260	195	115 034.7	23	20	15	52.3
12	240	180	90 477.8				

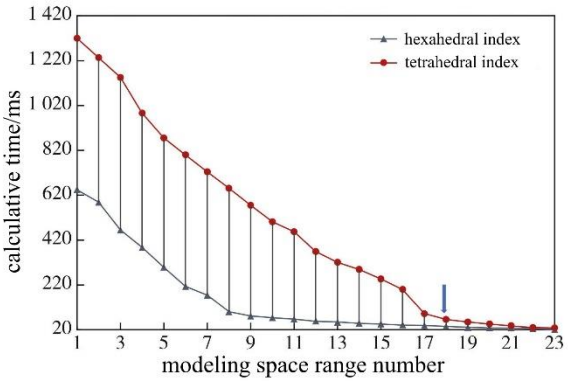

Figure 8: Comparison of time-consuming for voxel construction in two modes

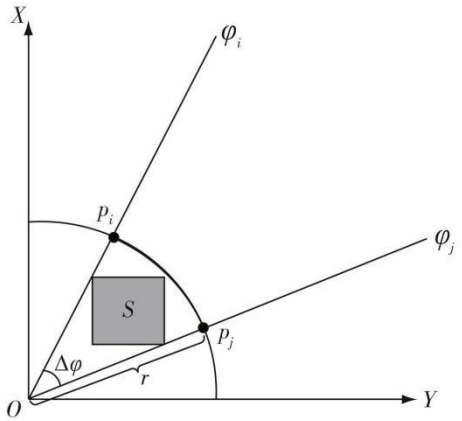

Figure 9: The algorithm realizing the XY plane of the selected spatial range

3.3 Hexahedral index pattern topology construction

The hexahedral index model uses trapezoidal hexahedral as the basic volume unit to construct a three-dimensional iso-surface connection topology. Set the vertex Index to represent the relationship between the trapezoidal hexahedral vertex $V_i(i = 0,1,\cdots,7)$ and the iso-surface value α, and the structure is shown in Figure 10.

Each vertex is represented by 1 bit. $V_i = 1$ when the vertex value is less than or equal to α, $V_i = 0$ when the vertex value is greater than α. The eight vertices of the trapezoidal hexahedral can be greater than α or less than or equal to α, so the Index range is 0 to 255. For example, an Index value of 1 indicates that the V_0 vertex is 1 and the other vertices are 0.

The structural Index table IntersectEdge stores the intersecting edge between iso-surface and voxel, and uses index value to index. Each element in the Intersect Edge array uses 2 bytes to identify whether the 12 edges intersect with the iso-surface. Each edge occupies 1 bit, 0 represents disjunction, 1 represents intersection, and the highest 4 bits are fixed as 0. For example, edges E_0, E_3, E_8 have intersecting points with iso-surface, IntersectEdge[Index] = 0000000100001001.

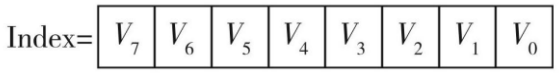

Figure 10: Diagram of vertex index byte structure

The triangular surface configuration table Triangle stores the number of triangles connected to equivalent points in voxels and the connection mode, and uses Index value for index. Figure 11 is the schematic diagram of the triangular surface configuration table. Each element of the Triangle array is a one-dimensional array of length 16, and each value in the array is the number of the edge where the equivalent point is located. Every 3 values constitute a triangular surface.

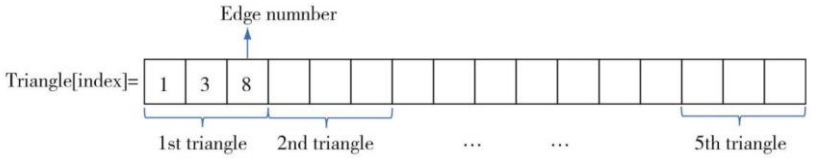

Figure 11: Diagram of triangular patch configuration table

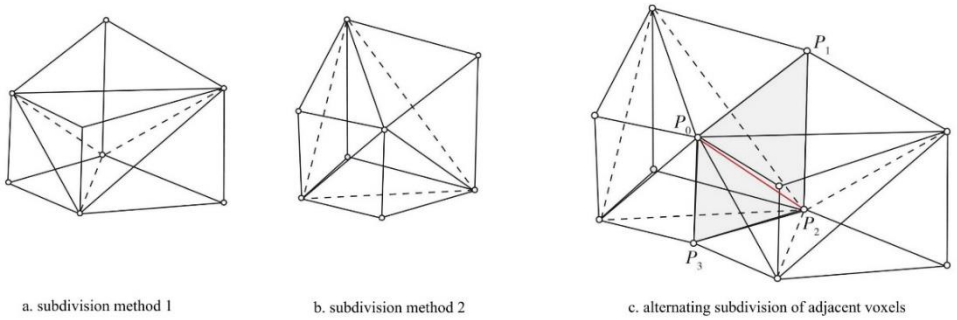

Figure 12: Partition of adjacent trapezoid hexahedral (solid lines represent lines drawn on the outside of the voxel, dashed lines represent lines drawn on the inside of the voxel, and red dotted line represents the division line on the common surface)

3.4 Topology construction of tetrahedral index pattern

Figure 12 is the trapezoidal hexahedral partition diagram, Figure 12a and 12b are the two ways to divide the trapezoidal hexahedral into five tetrahedra. Since the tetrahedral obtained by the two partitioning methods are different, in order to avoid

the inability to splice the triangular surfaces on the common surfaces of the adjacent trapezoidal hexahedral, the partitioning method with alternating intervals as shown in Figure 12c was adopted when the adjacent voxels were divided. After the adjacent trapezoidal hexahedral are alternately divided, the common surfaces formed by the vertices P_0, P_1, P_2, P_3 are divided into two triangles, $\Delta P_0P_2P_3$ and $\Delta P_0P_1P_2$, which are one face of the tetrahedral. On the one hand, the number of polyhedrons obtained by this voxel partitioning method is small, and on the other hand, the stitching consistency on the common surface is ensured.

Tetrahedral index model uses tetrahedral as voxels to construct iso-surface. The tetrahedral has four vertices, so the vertex Index V_4 through V_7 is fixed to 0. It can be seen from the vertex state that there are $2^4 = 16$ kinds of intersection relations between tetrahedral edge and iso-surface, so the length of the edge table IntersectEdge and the triangular surface configuration table Triangle are both 16. Each element of the IntersectEdge array uses a byte to mark whether the 6 edges of the tetrahedral intersect with the iso-surface. Each element of the Triangle becomes a one-dimensional array of length 9, with the structure consistent with the hexahedral index pattern.

3.5 Calculate the intersection coordinates

According to the two vertex coordinates of the intersecting edges and their normal vectors, the coordinates and normal vectors of the intersecting points are determined by linear interpolation. If the reflectance of the two endpoints $p_1 = (x_1, y_1, z_1)$ and $p_2 = (x_2, y_2, z_2)$ of the edge where the intersection point is located is R_1 and R_2, and the iso-surface value is c, then the coordinates of the equivalent point $p = (x, y, z)$ are

$$P(x, y, z) = P_1(x_1, y_1, z_1) + \frac{c-R_1}{R_2-R_1}\big(P_2(x_2, y_2, z_2) - P_1(x_1, y_1, z_1)\big). \tag{2}$$

for any point of the iso-surface, the vector direction of its gradient is the normal vector of the iso-surface at that point. The gradient of the vertex is calculated according to formula (3) and the normal vector at the intersection is obtained by linear interpolation of formula (4). Where the function $R = (x, y, z)$ represents the reflectance at coordinates x, y, z, $\Delta x, \Delta y$ and Δz are the voxel side lengths in three directions.

$$\begin{cases} N_x(x, y, z) = \frac{R(x+1,y,z)-R(x-1,y,z)}{2\Delta x}, \\ N_y(x, y, z) = \frac{R(x,y+1,z)-R(x,y-1,z)}{2\Delta y}, \\ N_z(x, y, z) = \frac{R(x,y,z+1)-R(x,y,z-1)}{2\Delta z}, \end{cases} \tag{3}$$

$$N(x, y, z) = N\big(N_x, N_y, N_z\big) = N_1(x_1, y_1, z_1) + \frac{c-R_1}{R_2-R_1}\big(N_2(x_2, y_2, z_2) - N_1(x_1, y_1, z_1)\big). \tag{4}$$

according to the coordinates of intersection points and the normal vector, the three-dimensional iso-surface is drawn according to the intersection connection method given by the Triangle configuration table.

4 Experiment and analysis

In order to test the effect of radar 3D modeling algorithm, the three algorithms in Table 2 were used to conduct 3D modeling of radar echoes in the space range of 33.6°~34.2°N and 119.5°~119.8°E at 06:18 UTC on June 23, 2016. The test computer is a dual-core processor, the main frequency is 2.50 GHz, and the memory is 4 GB.

4.1 Algorithm performance analysis

Table 3 shows the number of triangular surfaces and operation time obtained by running each test algorithm for 10 times, in which the operation time is taken as the average value of 10 times. In the same spatial range, the number of triangular surfaces obtained by the hexahedral index model algorithm is about 53% that of the traditional three-dimensional modeling algorithm, which significantly reduces the operation time. Although the tetrahedral index pattern algorithm has a significant increase in the number of triangular surfaces compared with the hexahedral index pattern algorithm, it is still less than the traditional modeling algorithm, and the calculation time is 0.7 s less than the traditional algorithm. Therefore, the MTPD algorithm is superior to the traditional radar 3D modeling algorithm in computational efficiency.

Table 2: Introduction of test algorithms

test algorithm name	radar data	voxel shape	subdivision
traditional three-dimensional modeling algorithm	grid point data with a spatial resolution of 1km	cube	No
hexahedral index mode	original base data	trapezoidal hexahedron	No
tetrahedral index mode	original base data	trapezoidal hexahedron	Yes

Table 3: Performance comparison of test algorithms

test algorithm	number of triangular facets/piece	computing time/s
traditional three-dimensional modeling algorithm	790 987	3.04
hexahedral index mode	415 754	1.14
tetrahedral index mode	708 227	2.34

4.2 Analysis of 3D modeling results

Figure 13 shows the 3D modeling effect of radar reflectivity of each test algorithm. From the overall effect, the three-dimensional structure of echo obtained by MTPD algorithm (Figure 13b and 13c) is very close to that obtained by traditional algorithm (Figure 13a), and the small differences are acceptable in practical application, which also verifies the correctness of MTPD algorithm. In order to further observe the three-dimensional structure details of radar echoes, the reflectance of 55~56 dBz was

selected for grid display (Figure 14). It can be seen that the hexahedral index mode (Figure 14b) and tetrahedral index mode (Figure 14c) in the MTPD algorithm construct the three-dimensional structure of radar echo with fewer triangular surfaces, which is almost the same as that of the traditional three-dimensional modeling algorithm (Figure 14a). The hexahedral index mode and the traditional three-dimensional modeling algorithm have obvious holes in the network structure (Figure 14a and 14b), while the tetrahedral index mode (Figure 14c) splices the triangular surfaces continuously in this region, completely avoiding the problem of holes between adjacent surfaces without subdivision, and the three-dimensional structure is more continuous and more accurate.

Based on the above experimental results, the MTPD algorithm produces fewer triangular surfaces and takes significantly less time in 3D modeling than the traditional algorithm. Hexahedral index model has the fastest computation speed and tetrahedral index model has the best continuous modeling results. Therefore, for the application scenarios of 3D model with high timeliness requirements or large-scale weather analysis such as typhoon, the hexahedral index model can get the ideal effect, while the tetrahedral index model is used in the scenario where the structural details of radar echoes need to be observed. In practical application, MTPD will automatically select the index mode according to the rectangular S-area of the modeling range according to the applicable mode determination criteria described in 2.2.

5 Algorithm Application

WebGL is a browser-side 3D drawing standard, which can realize Web 3D modeling and interactive display without any browser plug-in, and improve the graphics rendering speed through underlying hardware acceleration [21]. Three.js is an open-source framework that encapsulates the underlying code of WebGL, with built-in many commonly used objects and tools in 3D graphics programming. It is open and easy to use. In this paper, a Doppler weather radar visualization platform is developed by using this framework, and the proposed radar base data moving trapezoidal polyhedron 3D modeling algorithm is implemented in the browser. At the same time, vector map scaling interaction, multi-layer control, radar basic reflectivity and velocity map single and animation display, vertical section and other functions are realized.

A severe convective weather occurred in Nanjing on March 20, 2019. Figure 15a shows the observation results of 3.4° elevation Angle of SA Doppler weather radar at 05:42 (UTC). There are obvious three-body scattering "spikes" in the red box area, and the reflectivity factor of the strongest echo is greater than 60 dBz. Figure 15b shows the three-dimensional structure of radar reflectivity in the red box area of Figure 15a. The top height of the 25dBz echo is about 10km. It can be seen from the reflectance three-dimensional structure of more than 40 dBz (Figure 15c) that the

center of the strong echo of more than 65 dBz is overhanging in the region of more than 5 km, and the presence of vertical wind shear leads to the tilt of the overhanging structure. The reflectance factor of 3.4° elevation at 06:06 (UTC) (Figure 15d) is significantly reduced. The strongest echo drops to about 50 dBz. The three-dimensional structure of radar reflectivity in the red box area in Figure 15d (Figure 15e) shows that the top height of the 25 dBz echo is reduced to 8 km. From the reflectivity three-dimensional structure of 40 to 60 dBz (Figure 15f), it can be seen that the height of the center of the strong echo drops to about 3 km, and the echo overhanging structure has disappeared. At 06:08 (UTC), a hail of 1 cm diameter was observed in Lishui area. The three-dimensional structure of radar reflectance clearly reflects the development process of the hail system, which can provide a direct means for forecasters to intuitively and comprehensively understand the distribution and internal structure of the space echo.

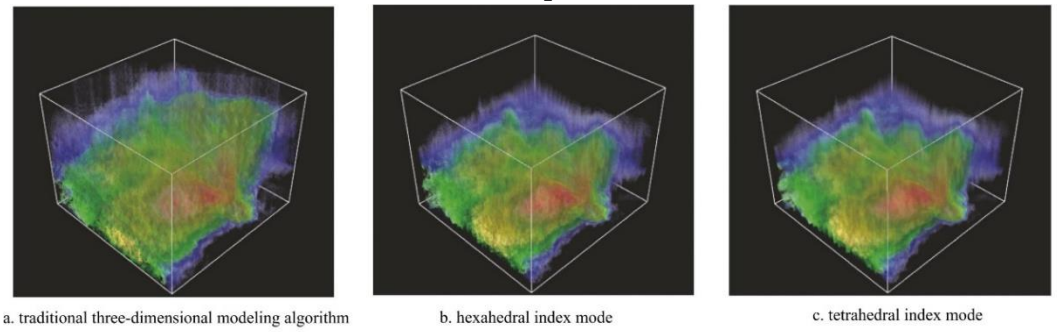

Figure 13: Comparison of 3D modeling results of three test algorithms

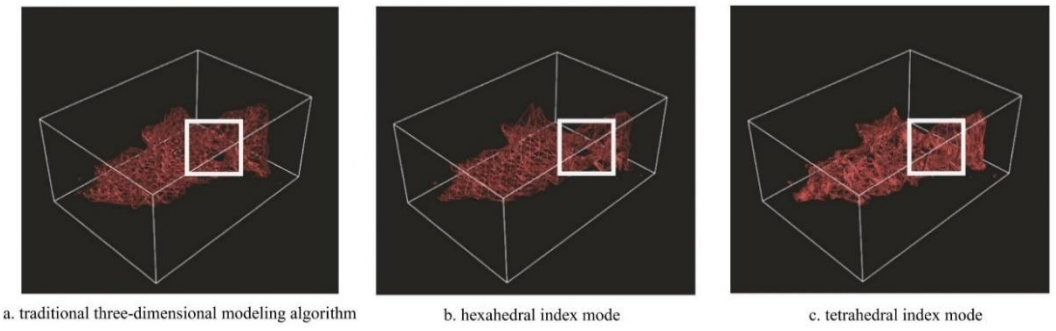

Figure 14: Comparison of 3D netlike structure of 55-56 dBz reflectivity among three test algorithms

6 Conclusions and discussions

In this paper, according to the characteristics of Doppler weather radar base data, a moving trapezoidal polyhedron three-dimensional modeling algorithm (MTPD) based on radar original base data is proposed, and a radar reflectivity modeling comparison experiment is conducted with the traditional radar 3D modeling algorithm. Based on MTPD algorithm, a three-dimensional visualization platform of Doppler weather radar is developed using WebGL technology. The main conclusions are as follows.

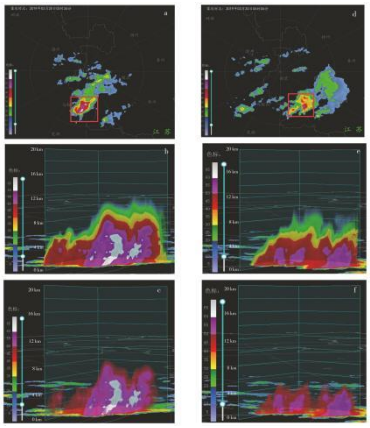

Figure 15: Results of 2D and 3D modeling of Nanjing radar at 05:42 (UTC) and 06:06 (UTC) on March 20, 2019 a. Basic reflectivity at 05:42 (UTC) and 3.4° elevation; b. 3D modeling results of the red box area in (a) ; c. 3D modeling results with basic reflectivity greater than 40 dBz of the red box area in (a) ; d. basic reflectivity at 06:06 (UTC) and 3.4° elevation; e. 3D modeling results of the red box area in (d) ; and f. 3D modeling results with basic reflectance of 40 to 60 dBz of the red box area in (d)

1) Compared with the traditional radar 3D modeling algorithm based on radar 3D grid data, the MTPD algorithm's 3D modeling results are highly similar to those of the traditional algorithm in the same spatial range, and the calculation time is reduced by 1.9 s (hexahedral index mode) and 0.7 s (tetrahedral index mode), respectively. The results show that the algorithm can effectively improve the efficiency without losing the accuracy.

2) Tetrahedral index mode solves the problem of holes caused by discontinuity of radar three-dimensional structure in hexahedral index mode by alternately dividing trapezoidal hexahedral into 5 tetrahedral in 2 different ways, and the display effect is more accurate. The tetrahedral index model can be used to analyze the three-dimensional structure of radar echoes in small scale severe convective weather like tornado. The hexahedral index mode is the fastest, which is suitable for the service scenario of displaying large-scale weather such as typhoon in the three-dimensional structure of the whole radar echo.

3) The algorithm frames the space range on the two-dimensional plane of the radar for 3D modeling. When the rectangular area of the frame is less than or equal to 17 959 km2, the tetrahedral index mode is selected, and when the rectangular area is greater than 17 959 km2, the hexahedral index mode is selected. The calculation efficiency and the accuracy of modeling results were balanced by selecting different models.

4) The three-dimensional visualization platform of Doppler weather radar based on WebGL realizes the two-dimensional and three-dimensional interactive display of radar echoes combined with geographic information, making the spatial analysis of radar echoes more convenient and intuitive.

The MTPD algorithm also needs to be further optimized. The tetrahedral index mode increases the number of volume units to be processed by splitting voxels and also increases the number of triangular surfaces. Compared with the hexahedral index mode, the algorithm takes more time. In the next step, parallel computing technology will be introduced to extract 3D iso-surface synchronously from the five tetrahedral obtained by subdivision, and optimize the storage structure of the resulting triangle slices, so as to ensure the accuracy of 3D modeling and improve the algorithm efficiency of the tetrahedral index model.

Acknowledgments

This work is supported by the Small Infrastructure Project of China Meteorological Administration (Grant No. QJ-2017006) and Key Project of Jiangsu Meteorological Bureau (Grant No. KZ201904).

Conflicts of Interest

The authors declare no conflict of interest.

References

[1] H. Wen, L. P. Liu, and Y. Zhang, Improvements of ground clutter identification algorithm for Doppler weather radar, *Plateau Meteorol.*, 2017, 36(3): 736-749.
[2] Y. J. Xiao, An algorithm of recognizing automatically MARC signature using the Doppler weather radar volume scanning data, *Plateau Meteorol.*, 2018, 37(1): 264-274.
[3] X. Y. Huang, J. Peng, Z. Y. Mao, et al., Analysis of algorithm for identifying active jamming echo from Doppler weather radar, *Meteorol. Monthly*, 2019, 45(3): 371-380.
[4] X. D. Yu, and Y. G. Zheng, Advances in severe convective weather research and operational service in China, *Acta Meteorol. Sinica*, 2020, 78(3): 391-418.
[5] H. H. Liang, P. Y. Zhang, F. Niu, et al., China operational weather radar data processing system, *Q. J. Appl. Meteorol.*, 2002, 13(6): 749-754.
[6] S. Y. Liu, J. Sun, W. D. Guo, et al., A dealing and graphic system for Doppler radar data, *Meteorol. Monthly*, 2004, 30(7): 44-46,2.
[7] J. Zhang, S. D. Zhang, and H. Dai, Design of a severe weather monitoring and warning system for Doppler weather radar PUP products, *Torrential Rain Disasters*, 2018, 37(5): 486-492.
[8] A. Ernvik. 3D visualization of weather radar data, Linköping, Sweden: *Linköping University*, 2002.
[9] P. Kristof, B. Benes, C. X. Song, et al., A system for large-scale visualization of streaming Doppler data, 2013 IEEE International Conference on Big Data, October 6-9, 2013, Silicon Valley, CA, USA. *IEEE*, 2013: 33-40.

[10] A. Moreno, A. Galdós, A. Mujika, et al., Visual analytics of multi-sensor weather information georeferenciation of Doppler weather radar and weather stations, International Conference on Information Visualization Theory and Applications, January 5-8, 2014, Lisbon, Portugal, *IEEE*, 2014: 329-336.
[11] Y. J. Xiao, and L. P. Liu, Study of methods for interpolating data from weather radar network to 3-D grid and mosaics, *Acta Meteorol. Sinica*, 2006, 64(5): 647-657.
[12] Z. Q. Zhang, L. P. Liu, M. Y. Xie, et al., A display system of CINRAD 3D mosaic products, *Meteorol. Monthly*, 2007, 33(9): 19-24,129.
[13] X. J. Luo, Design of Doppler weather radar production terminal and its echoes 3D visualization method, Nanjing: *Nanjing University of Information Science & Technology*, 2008.
[14] C. Y. Han, The three-dimensional reconstruction based on meteorological radar data, Tianjin: *Tianjin University*, 2012.
[15] H. Y. Wang, L. P. Liu, G. L. Wang, et al., Development and application of the Doppler weather radar 3-D digital mosaic system, *J. Appl. Meteorol. Sci.*, 2009, 20(2): 214-224.
[16] T. Qiu, J. L. Liu, and X. Li, Development and application of OPENGL-based 3D display visualization system in weather radar networking, *Meteorol. Sci. Technol.*, 2015, 43(5): 833-838.
[17] Y. J. Liu, S. S. Gu, Y. H. Zhou, et al. Comparison of CINRAD/SA volume coverage patterns on algorithms output, *Meteorol. Monthly*, 2006, 32(1): 44-50.
[18] X. Q. Wang, Q. H. Ni, Z. Z. Tong, et al., Interpolating and filling methods for processing basic data of new generation weather radar, *Meteorol. Sci. Technol.*, 2007, 35(sup1): 61-64,94.
[19] S. B. Bi, G. J. Zhang, R. T. Hou, et al., Comparing research on 3D modeling technology & its implement methods, *J. Wuhan Univ. Technol.*, 2010, 32(16): 26-30,83.
[20] L. R. Wang, and L. R. Wang, Influence of horizontal distance and altitude on radar rainfall estimation and its correction, *Meteorol. Monthly*, 2017, 43(9): 1152-1159.
[21] N. Rego, and D. Koes. 3D mol. js: molecular visualization with WebGL, *Bioinformatics*, 2015, 31(8): 1322-1324.